Strong *in vitro* and *vivo* cytotoxicity of three new cobalt(II) complexes with 8-methoxyquinoline

Yu-Feng Wang,[a] Ji-Xia Tang,[b] Zai-Yong Mo,[c,*] Juan Li,[a] Fu-Pei Liang,[a,d,*] Hua-Hong Zou[a,*]

[a]*State Key Laboratory for Chemistry and Molecular Engineering of Medicinal Resources, School of Chemistry and Pharmacy of Guangxi Normal University, Guilin 541004, P. R. China. gxnuchem@foxmail.com (H.-H. Zou), fliangoffice@yahoo.com (F.-P. Liang).*

[b]*School of Foreign Language and International Business, Guilin University of Aerospace Technology, Guilin, 541004, P. R. China.*

[c]*Guangxi Key Lab of Agricultural Resources Chemistry and Biotechnology, College of Chemistry and Food Science, Yulin Normal University, 1303 Jiaoyudong Road, Yulin 537000, PR China. xdmozy@163.com (Z.-Y. Mo).*

[d]*Guangxi Key Laboratory of Electrochemical and Magnetochemical Functional Materials, College of Chemistry and Bioengineering, Guilin University of Technology, Guilin 541004, P. R. China.*

*E-mail (Corresponding author): gxnuchem@foxmail.com (H.-H. Zou), fliangoffice@yahoo.com (F.-P. Liang), xdmozy@163.com (Z.-Y. Mo).

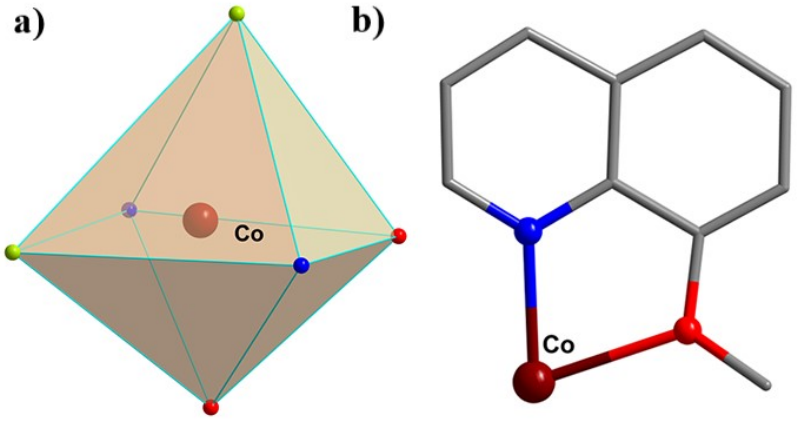

Figure S1. (a) Metal ion coordination configuration diagram; (b) ligand coordination pattern diagram.

Table S1. Crystallographic data of **CoCl**, **CoBr** and **CoI**.

Complex	**CoCl**	**CoBr**	**CoI**
Formula	$C_{20}H_{18}Cl_2CoN_2O_2$	$C_{20}H_{18}Br_2CoN_2O_2$	$C_{20}H_{18}I_2CoN_2O_2$
Formula weight	448.19	537.11	631.09
T (K)	300.71(10)	300.81(10)	300.99(10)
Crystal system	Triclinic	Triclinic	Triclinic
Space group	*P*Error!	*P*Error!	*P*Error!
a (Å)	7.5841(5)	7.7025(3)	7.8982(3)
b (Å)	9.5978(6)	9.6198(3)	11.2700(7)
c (Å)	14.5635(9)	14.7802(5)	12.5221(5)
α (°)	81.650(5)	80.313(3)	74.391(4)
β (°)	78.574(5)	75.682(3)	88.386(3)
γ (°)	67.050(6)	67.038(4)	77.493(4)
V (Å^3)	954.11(10)	973.89(6)	1047.51(9
Z	2	2	2
D_c (g cm^{-3})	1.560	1.832	2.001
μ (mm^{-1})	1.197	5.002	3.783
Reflns coll.	8340	9958	18911

Unique reflns	3350	3442	3694
R_{int}	0.0428	0.0939	0.0359
$^{a}R_1[I \geq 2\sigma(I)]$	0.0648	0.0314	0.0219
$^{b}wR_2$(all data)	0.2096	0.0766	0.0564
GOF	1.087	1.075	1.118

Table S2. Selected bond lengths (Å) and angles (°) of **CoCl**, **CoBr** and **CoI**.

Bond lengths (Å)					
CoCl		**CoBr**		**CoI**	
Co1–Cl1	2.3472(19)	Co1–Br1	2.5127(6)	Co1–I1	2.7320(5)
Co1–Cl2	2.3525(16)	Co1–Br2	2.5004(6)	Co1–I2	2.7167(5)
Co1–O1	2.277(4)	Co1–O1	2.298(2)	Co1–O1	2.269(2)
Co1–O2	2.314(4)	Co1–O2	2.259(2)	Co1–O2	2.282(2)
Co1–N1	2.124(5)	Co1–N1	2.124(3)	Co1–N1	2.102(2)
Co1–N2	2.134(5)	Co1–N2	2.117(3)	Co1–N2	2.103(2)
Bond angles (°)					
CoCl		**CoBr**		**CoI**	
Cl1–Co1–Cl2	105.82(7)	Br1–Co1–Br2	105.82(7)	I1–Co1–I2	107.50(16)
O1–Co1–O2	76.94(15)	O1–Co1–O2	77.23(10)	O1–Co1–O2	78.16(9)
O1–Co1–Cl1	93.91(12)	O1–Co1–Br1	86.61(7)	O1–Co1–I1	86.80(6)
O1–Co1–Cl2	157.50(12)	O2–Co1–Br1	159.53(7)	O1–Co1–I2	164.71(6)
O2–Co1–Cl1	164.05(12)	O1–Co1–Br2	164.55(7)	O2–Co1–I1	163.45(6)
O2–Co1–Cl2	86.01(11)	O2–Co1–Br2	92.79(7)	O2–Co1–I2	88.19(6)
N1–Co1–O1	72.98(15)	N2–Co1–O1	94.98(9)	N2–Co1–O1	94.24(16)
N1–Co1–O2	96.44(16)	N2–Co1–O2	73.74(9)	N2–Co1–O2	73.74(9)
N1–Co1–N2	164.87(17)	N1–Co1–N2	164.78(11)	N1–Co1–N2	160.70(10)
N1–Co1–Cl1	93.23(14)	N1–Co1–Br1	92.61(8)	N1–Co1–I1	92.25(7)
N1–Co1–Cl2	94.81(13)	N1–Co1–Br2	96.74(8)	N1–Co1–I2	99.00(7)
N2–Co1–Cl1	95.76(14)	N2–Co1–Br1	95.55(8)	N2–Co1–I1	99.37(6)
N2–Co1–Cl2	94.42(13)	N2–Co1–Br2	93.46(8)	N2–Co1–I2	92.18(7)

N2–Co1–O1	94.24(16)	N2–Co1–O1	94.98(9)	N1–Co1–O1	74.48(9)
N2–Co1–O2	72.27(16)	N2–Co1–O2	73.74(9)	N1–Co1–O2	90.38(9)

Table S3. *SHAPE* analysis of the Co^{II} ion in **CoCl**.

Label	Shape	Symmetry	Distortion(°)
HP-6	D_{6h}	Hexagon	30.388
PPY-6	C_{5v}	Pentagonal pyramid	22.485
OC-6	O_h	Octahedron	2.226
TPR-6	D_{3h}	Trigonal prism	12.154
JPPY-5	C_{5v}	Johnson pentagonal pyramid (J2)	27.284

Table S4. *SHAPE* analysis of the Co^{II} ion in **CoBr**.

Label	Shape	Symmetry	Distortion(°)
HP-6	D_{6h}	Hexagon	49.272
PPY-6	C_{5v}	Pentagonal pyramid	39.141
OC-6	O_h	Octahedron	34.757
TPR-6	D_{3h}	Trigonal prism	41.275
JPPY-5	C_{5v}	Johnson pentagonal pyramid (J2)	42.984

Table S5. *SHAPE* analysis of the Co^{II} ion in **CoI**.

Label	Shape	Symmetry	Distortion(°)
HP-6	D_{6h}	Hexagon	51.511
PPY-6	C_{5v}	Pentagonal pyramid	41.010
OC-6	O_h	Octahedron	36.700
TPR-6	D_{3h}	Trigonal prism	44.171
JPPY-5	C_{5v}	Johnson pentagonal pyramid (J2)	44.523

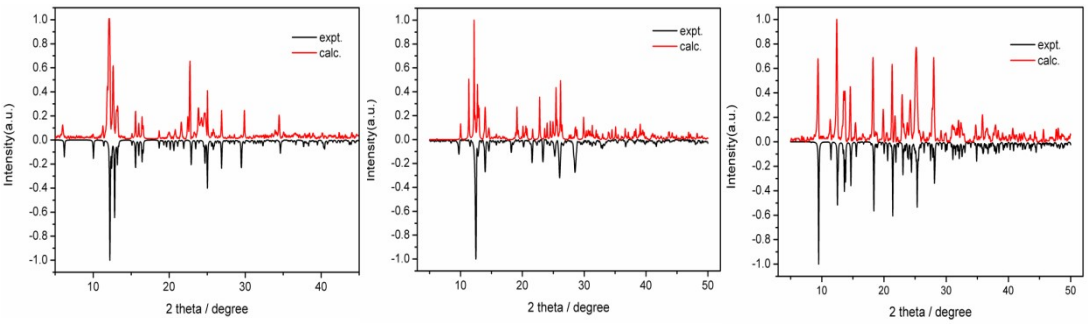

Figure S2. Powder diffraction pattern (PXRD) of **CoCl**, **CoBr** and **CoI**.

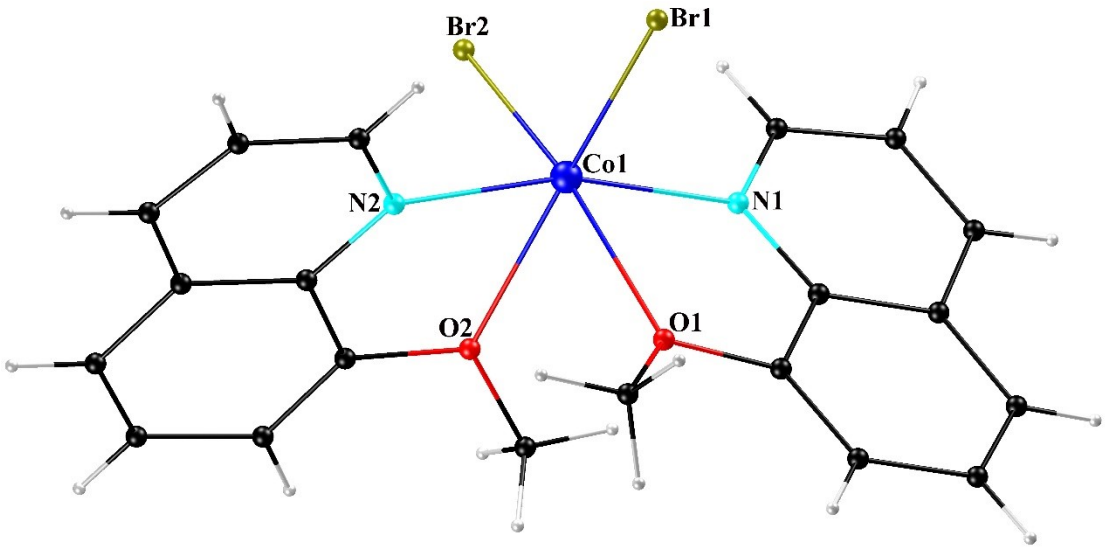

Figure S3. Structure diagram of **CoBr**. Bond distances (Å) of Co-Br: Co1–Br1, 2.5127(6); Co1–Br2, 2.5004(6).

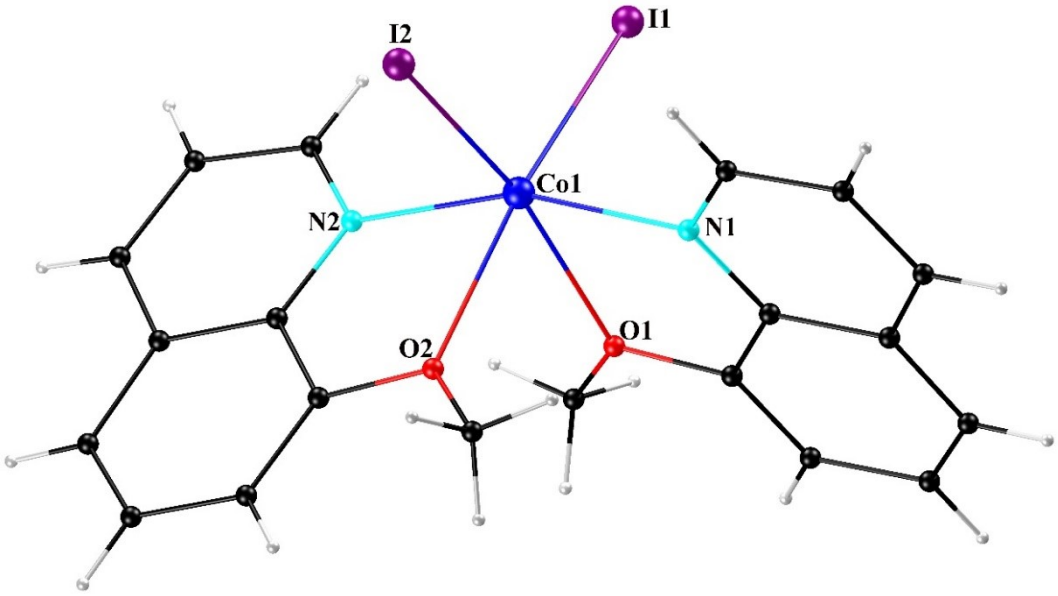

Figure S4. Structure diagram of **CoI**. Bond distances (Å) of Co-I: Co1–I1, 2.7320(5); Co1–I2, 2.7167(5).

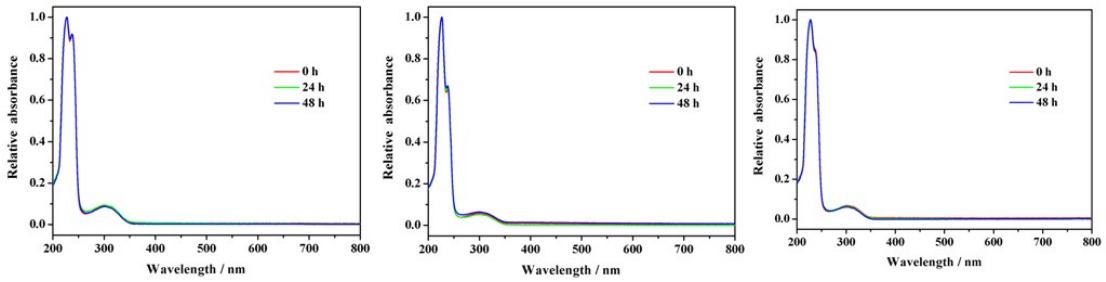

Figure S5. UV-Vis absorption spectra of **CoCl**, **CoBr** and **CoI** (2.0×10^{-5} M) in Tris-NaCl-HCl solution in the time course 0 h, 24 h and 48 h, respectively.

Table S6. The tumor volume in treated and non-treated mice from the date of surgery to the study end point in the SK-OV-3 xenograft model.

	mg/kg	1day	3d			5d			7d		
		Tumor Volume (mm^3)	Tumor Volume (mm^3)	RTV	T/C%	Tumor Volume (mm^3)	RTV	T/C%	Tumor Volume (mm^3)	RTV	T/C %
control	-	90.6±11.8	161.1±26.3	1.791±0.311	100.0	320.8±45.7	3.555±0.417	100.0	511.1±90.6	5.639±0.589	100.0
CoI	15 mg/kg	91.2±19.7	147.9±30.4	1.625±0.072	91.8	257.8±52.5	2.839±0.227**	80.4	382.1±78.3*	4.205±0.343**	74.8
CoCl	15 mg/kg	91.0±12.1	141.0±23.2	1.560±0.263	87.5	193.4±33.5**	2.135±0.343**	60.3	268.6±50.5**	2.969±0.556**	52.6

	mg/kg	9d			11d			13d		
		Tumor Volume (mm^3)	RTV	T/C %	Tumor Volume (mm^3)	RTV	T/C%	Tumor Volume (mm^3)	RTV	T/C%
control	-	702.9±131.3	7.752±0.927	100.0	991.6±211.2	10.915±1.476	100.0	1294.1±314.5	14.215±2.197	100.0
CoI	15 mg/kg	468.4±99.7**	5.150±0.363**	66.6	564.8±123.9**	6.207±0.570**	57.0	687.1±140.6**	7.572±0.736**	53.1
CoCl	15 mg/kg	337.8±64.5**	3.726±0.663**	48.1	432.8±69.4**	4.789±0.775**	43.6	506.2±64.8**	5.597±0.696**	39.1

	mg/kg	15d		
		Tumor Volume (mm^3)	RTV	T/C%
control	-	1578.1±407.3	17.316±2.973	100.0
CoI	15 mg/kg	778.0±153.9**	8.572±0.729**	49.3
CoCl	15 mg/kg	592.7±86.8**	6.531±0.737**	37.6

* p <0.05, ** p <0.01, p *vs* vehicle control (5.0% v/v DMSO/ saline vehicle).

Table S7. Average body weight in treated and non-treated mice from the date of surgery to the study end point in the A549/DDP xenogfart model.

	mg/kg	1 d	3 d	5 d	7 d	9 d	11 d	13 d	15 d
control	-	21.2±0.5	21.3±0.6	21.5±0.6	21.6±0.6	21.9±0.6	22.1±0.6	22.4±0.6	22.5±0.6
CoI	15 mg/kg	21.1±0.5	21.2±0.5	21.3±0.5	21.5±0.5	21.7±0.5	21.9±0.4	22.2±0.5	22.3±0.5
CoCl	15 mg/kg	21.0±0.4	21.1±0.4	21.1±0.4	21.3±0.4	21.5±0.4	21.7±0.4	21.9±0.4	22.0±0.4

* p <0.05, ** p <0.01, p *vs* vehicle control (5.0% v/v DMSO/ saline vehicle).

Table S8. In Vivo Anticancer Activity of **CoCl** (15 mg/kg/2days) and **CoI** (15 mg/kg/2days) toward SK-O-V-3 Tumor Xenograft.

	mg/kg	number of animal experiments (before dosing)	number of animal experiments (experiment end)	average tumor weight (mean ± SD, g)	inhibition of tumor growth (%)
control	-	6	6	1.343±0.397	—
CoI	15 mg/kg	6	6	0.688±0.087**	48.8
CoCl	15 mg/kg	6	6	0.536±0.084**	60.1

* p <0.05, ** p <0.01, p *vs* vehicle control (5.0% v/v DMSO/ saline vehicle).

Experimental

The detailed procedures of the in vitro and in vivo experimental methods were performed as reported by Zhang and Liang.[1-3]

1.1 Materials

The Tris, gel loading buffer, RNase A, 2-nitrobenzoic acid and propidium iodide (PI) were purchased from Sigma. The antibody beclin1, p62, and LC3 were purchased from Abcam. The human cell lines SK-OV-3/DDP, SK-OV-3 and HL-7702 were obtained from the Shanghai Institute for Biological Science (China).

1.2 Instruments

Elemental analyses (C, H and N) were carried out on a PerkinElmer series II CHNS/O 2400 elemental analyzer. ESI-MS spectra was performed on Thermofisher Scientific Exactive LC-MS spectrometer (Thermal Elctronic, USA). The MTT assay was performed on M1000 microplate reader (Tecan Trading Co. Ltd., Shanghai, China). Apoptosis assay and the cellular localization behavior analysis were recorded on confocal microscopy (Olympus FV300, Japan).

1.3 Cell Culture

The each cell culture was maintained in RPMI-1640 medium supplemented with 10.0% fetal bovine serum (FBS), 100.0 U/mL penicillin, and 100.0 μg/mL streptomycin in 25.0 cm^2 culture flasks at 37 °C in a humidified atmosphere with 5% CO_2. All the cells to be tested in the following assays had a passage number of 5.0.

1.4 MTT assays

The each cell line was seeded in 96 well plates at the density of 8000 cells per well for 24 h, then incubated with different concentrations of **CoCl**, $CoCl_2 \cdot 6H_2O$, MQL, CoI_2, **CoBr**, $CoBr_2$ and **CoI** for 24.0 h, and the cell medium was discarded and MTT (1.0 mg/mL) was added. After 4.0 h later, MTT solution was removed and DMSO was added. And obtained the results by a M1000 microplate reader (Tecan Trading Co. Ltd., Shanghai, China) at 570 nm[1-3].

1.5 Apoptotosis assay

Annexin V-FITC staining of the membranes was performed by Annexin-V APC and 7-AAD. The SK-OV-3/DDP cells were treated with **CoCl** and **CoI** at 0.32 μM for 24.0 h, and then the cells were stained with Annexin-V APC and 7-AAD double staining, and analyzed by flow cytometry.

1.6 Fluorescence imaging

Immunohistochemistry and fluorescence imaging was performed as previously described by Lee [4].

1.7 Western Blot

The SK-OV-3/DDP cells were incubated with **CoCl** and **CoI** at 0.32 μM for 24.0 h, and then the cells harvested from each well of the culture plates were lysed in 150 μL of extraction buffer consisting of 149.0 μL of RIPA lysis buffer and 1.0 μL of PMSF (100.0 mM). The suspension was centrifuged at 10 000 rpm at 4 °C for 10 min, and the supernatant (10.0μL for each sample) was loaded onto 10% polyacrylamide gel and then transferred to a microporous polyvinylidene difluoride (PVDF) membrane. Western blotting was performed using each anti-antibody, or anti-β-actin primary antibody and horseradish-peroxidase-conjugated anti-mouse or anti-rabbit secondary antibody. The protein bands were visualized using chemiluminescence substrate.

1.8 *In Vivo* Anticancer Activity

The SK-OV-3 cancer cells were harvested and injected subcutaneously into the right flank of nude mice with 6.0×10^6 cells in 200.0 μL of serum-free medium. When the xenograft SK-OV-3-tumor growth to the volume about 1000 mm^3, the mice were killed and the tumor tissue were cut into about 1.50 mm^3 small pieces, and then transplanted into the right flank of female nude mice, When tumors reach a volume of 90-100 mm^3 on all mice, the mice were randomized into vehicle control and treatment groups (n=6/group), received the following treatments: (a) vehicle control, 10.0% v/v DMSO/ saline vehicle, (b) **CoCl** at dose 15.0 mg/kg every two day (10% v/v

DMSO/saline), (c) **CoI** (15.0 mg/kg) by injected intraperitoneally every 2 days (q2d). The SK-OV-3 tumor volumes were determined every three days by measuring length (*l*) and width (*w*) and calculating volume, tumor volume and inhibition of tumor growth were calculated using formulas 1−3:[1-3]

Tumor volume: $V = (w^2 \times l)/2$ (1)

The tumor relative increment rate: $T/C\ (\%) = T_{RTV}/C_{RTV} \times 100\%$ (2)

inhibition of tumor growth: $IR(\%) = (W_c - W_t)/W_c \times 100\%$ (3)

Where w and l mean the shorter and the longer diameter of the tumor respectively; T_{RTV} and C_{RTV} was the RTV of treated group and control group respectively. (RTV: relative tumor volume, $RTV = V_t / V_0$); W_t and W_c mean the average tumor weight of complex-treated and vehicle controlled group respectively.

In addition, the SK-OV-3 xenograft mouse models were purchased from Changzhou cavens experimental animal Co., Ltd (Jiangsu, China, approval No. SCXK 2016-0010). The animal procedures were approved by Changzhou cavens experimental animal Co., Ltd (Jiangsu, China, approval No. SYXK 2017-0040). And all of the experimental procedures were carried out in accordance with the NIH Guidelines for the Care and Use of Laboratory Animals. Animal experiments were approved by Changzhou cavens experimental animal Co., Ltd ((Jiangsu, China).

1.9 Statistical Analysis

The experiments have been repeated from three to five times, and the results obtained are presented as means ± standard deviation (SD). Significant changes were

assesses by using Student's *t* test for unpaired data, and p values of <0.05 were considered significant.

References

1 (a) Y. Yang, Z. Zhou, Z.-Z. Wei, Q.-P. Qin, L. Yang, H. Liang, High anticancer activity and apoptosis- and autophagy-inducing properties of novel lanthanide(III) complexes bearing 8-hydroxyquinoline-N-oxide and 1,10-phenanthroline, *Dalton Trans.*, 2021, **50**, 5828–5834; (b) Z.-F. Wang, Q.-C. Wei, J.-X. Li, Z. Zhou, S.-H. Zhang, A new class of nickel(II) oxyquinoline-bipyridine complexes as potent anticancer agents induces apoptosis and autophagy in A549/DDP tumor cells through mitophagy pathways, *Dalton Trans.*, 2022, 51, 7154−7163.

2 (a) Q.-P. Qin, Z.-Z. Wei, Z.-F. Wang, X.-L. Huang, M.-X. Tan, H.-H. Zou, H. Liang, Imaging and therapeutic applications of Zn(II)-cryptolepine–curcumin molecular probes in cell apoptosis detection and photodynamic therapy, *Chem. Commun.*, 2020, **56**, 3999–4002.

3 (a) M.-X. Tan, Z.-F. Wang, Q.-P. Qin, B.-Q. Zou, H. Liang, Complexes of oxoplatin with rhein and ferulic acid ligands as platinum(IV) prodrugs with high antitumor activity, *Dalton Trans.*, 2020, **49**, 1613–1619; (b) Y.-Q. Gu, W.-Y. Shen, Q.-Y. Yang, Z.-F. Chen, H. Liang, Ru(III) complexes with pyrazolopyrimidines as anticancer agents: bioactivities and the underlying mechanisms, *Dalton Trans.*, 2022, **51**, 1333–1343.

4 J.-H. Lee, M. V. Rao, D.-S. Yang, P. Stavrides, E. Im, A. Pensalfini, C. Huo, P. Sarkar, T. Yoshimori and R. A. Nixon, Transgenic expression of a ratiometric autophagy probe specifically in neurons enables the interrogation of brain autophagy in vivo, *Autophagy*, 2019, **15**, 543–557.